

## Recent Progress in the Application of Polyoxometalates for Dye-sensitized/Organic Solar Cells

Tengling Ye,<sup>\*a</sup> Junhai Wang,<sup>a</sup> Guohua Dong,<sup>a,b</sup> Yanxia Jiang,<sup>a</sup> Chen Feng,<sup>a</sup> and Yulin Yang<sup>\*a</sup>

<sup>a</sup> MIIT Key Laboratory of Critical Materials Technology for New Energy Conversion and Storage, School of Chemistry and Chemical Engineering, Harbin Institute of Technology, Harbin, Heilongjiang 150001, China

<sup>b</sup> College of Chemistry and Chemical Engineering, Qiqihar University, Qiqihar, Heilongjiang 161006, China

At present, high efficiency and low fabrication cost are still the main goal that people pursuit for next-generation solar cells such as dye-sensitized solar cells (DSSCs) and organic solar cells (OPVs). Polyoxometalates (POMs), as an environmentally friendly material, are a type of stable, low cost and soluble oxide clusters with desirable features, including highly tunable structural properties, peculiar optoelectronic properties and excellent redox properties. Thus, during the recent years, POMs have been increasingly recognized as important building blocks for DSSCs and OPVs. In this review, the development of various molecular and hybrid materials derived from POMs is discussed with regard to the function in solar cells.

**Keywords** polyoxometalates, solar cell, optoelectronic devices, DSSC, OPV

### Introduction

Polyoxometalates (POMs) are a large group of metal-oxygen clusters derived from two or more inorganic acids by elimination of water. If the POM is condensed from the same inorganic acids, it is named iso-polyoxometalate; If not, the POM is named hetero-polyoxometalate. In general, POMs are composed of three or more transition metal oxyanions linked together by shared oxygen atoms to form a large, closed 3-dimensional framework.<sup>[1-3]</sup> The metal atoms that make up the framework are termed the addenda atoms and they are usually group 5 or group 6 transition metals in their high oxidation states, for example vanadium, niobium, tantalum, molybdenum, tungsten, etc. One or more hetero atoms (such as phosphorus, silicon, germanium, etc.) are enclosed in the center of the framework by sharing neighbouring oxygen atoms with transition metals.<sup>[4-6]</sup> Due to the possibilities of there being different combinations of transition metal atoms and hetero atoms, the structures of POMs are versatile. Six fundamental POM structures are shown in Figure 1, exhibiting Keggin, Dawson, Anderson, Waugh, Silverton and Lindqvist structures.<sup>[7,8]</sup> The above structures can be distinguished by the ratio of addenda atoms to hetero atoms. Keggin and Silverton structures are 1 : 12 series, Dawson and Waugh belong to 1 : 9 series, Anderson and Lindqvist are 1 : 6 series and 6 : 19 series, respectively.<sup>[9]</sup> Different metal cations and different valence ions can replace the absence of POMs, the formation of the derivatives not only expands the variety and structure of

POMs, but also improves the application area of POMs in practice.<sup>[10]</sup>

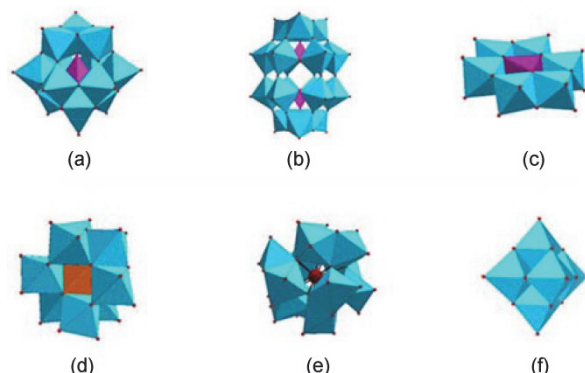


**Figure 1** Six typical structures of polyoxometalates: (a) Keggin, (b) Dawson, (c) Anderson, (d) Waugh, (e) Silverton, (f) Lindqvist.

POMs exhibit a rich diversity of properties owing to their structural versatility. The main physicochemical properties of POMs are as follows:

(1) The thermal stability of POMs is very good, the molecular size is large and the relative molecular weight is high ( $10^3$ – $10^4$ ).

(2) The composition elements are rich, non-toxic, tasteless, non-volatile, easy to be dissolved in oxygen-containing organic solvents such as water, ether, ethanol, acetone, etc.

(3) POMs have excellent redox properties and the majority of reduction shows blue, known as the "heteropoly blue", oxidation will restore color.<sup>[11]</sup> The redox

\* ytl@hit.edu.cn, ylyang@hit.edu.cn

Received April 14, 2016; accepted May 22, 2016; published online June 15, 2016.

potential can be easily tuned by adjusting the structure and composition of POMs.<sup>[12-14]</sup>

(4) Surfactants can effectively prevent the aggregation of POMs and obtain a variety of organic/inorganic hybrid materials.<sup>[15,16]</sup>

These special and superior physicochemical properties make POMs become the focus of research in many fields, such as catalyzed synthesis,<sup>[17,18]</sup> photocatalysis,<sup>[10]</sup> solar cell,<sup>[19,20]</sup> medicine,<sup>[21]</sup> electrochemistry,<sup>[22,23]</sup> geochemistry<sup>[24]</sup> and magnetism.<sup>[25]</sup>

Recently, the research of POMs in the field of solar energy conversion has been studied a lot, especially applied in dye-sensitized solar cells (DSSCs) and organic photovoltaic cells (OPVs) as a building block. Both of DSSCs and OPVs are the third generation of solar cells that have attracted considerable interests because of their relatively low cost, facile fabrication, high efficiency, and compatibility with flexible substrates.<sup>[26,27]</sup> The typical device structures of DSSCs and OPVs are shown in Figure 2. They are usually made up by a photoanode/electron extraction layer, dye/light absorption materials, electrolyte/hole transport layers, and a counter electrode/metal electrode.

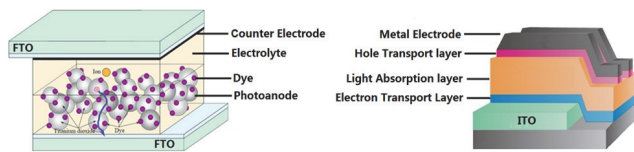


**Figure 2** Typical device structures of DSSCs and OPVs.

POMs possess good structure durability, solution processing in organic solvents, excellent redox properties, easy synthesis and low cost, especially the semiconductor characteristics. All of these unique properties make POMs be a novel and important building block for DSSCs and OPVs.<sup>[28-30]</sup> There are several existing reviews on POM-based materials for energy conversion, which mainly discussed the application in photocatalysis, catalyzed water oxidation, energy storage and photoelectric properties of POM-based thin films. The application in solar cells was seldom covered or did not update the latest progress.<sup>[30-38]</sup> In this review, we will mainly focus the topic on the application of POMs as a building block in the field of DSSCs and OPVs. We summarize the recent development of POM-based materials in the field of DSSCs and OPVs, furthermore, the working mechanism of POM-based materials in solar cells, problems and the research trends in the near future are also discussed.

## POMs for Solar Cells

### POMs based electronic interface materials

POMs can accept electrons readily and undergo reversible redox reactions without changing intact struc-

ture, which makes the POMs be a good electronic interface material in DSSCs or OPVs. Much attention has been paid to exploring new POMs as a photoanode or electron collection layer to improve the photoelectric conversion efficiency (PCE) of solar cells.

In 2009, Yoon and co-workers first applied  $\text{PW}_{12}\text{O}_{40}$ -incorporated  $\text{TiO}_2$  (PTA/ $\text{TiO}_2$ ) nanodisc film electrodes in DSSCs by simply spreading phosphotungstic acid (PTA) solution on the  $\text{TiO}_2$  nanodisc surface.<sup>[39]</sup> PTA/ $\text{TiO}_2$  nanodiscs film electrodes showed higher photoelectrochemical efficiency than  $\text{TiO}_2$  nanodisc film electrodes. POMs can serve as an electron mediator, which avoids most of backward electron transfer reactions and helps to enhance the PCE.

In 2013, Wang and co-workers successfully prepared PTA/ $\text{TiO}_2$  composite by combining sol-gel method and hydrothermal method. Electrochemical impedance spectroscopy and open circuit voltage decay curves showed that the POMs can effectively reduce the electron recombination and obtained a longer electron lifetime.<sup>[40]</sup> Subsequently, they tried to fabricate PTA/ $\text{TiO}_2$ -based interfacial layer for DSSCs by the layer-by-layer (LBL) method. The PCE at 100  $\text{mW} \cdot \text{cm}^{-2}$  of a (PTA/ $\text{TiO}_2$ )<sub>3</sub>-based DSSC was significantly enhanced by 54% compared with a DSSC with no treatment and by 20% compared with a  $\text{TiCl}_4$ -treatment DSSC. Enhanced performance was attributed to that PTA molecules promoted electrons to transfer from  $\text{TiO}_2$  to the external circuit and the recombination of electrons was efficiently suppressed by the PTA-based interfacial layer. The working mechanism was shown in Figure 3.<sup>[41]</sup> In 2015, Li and co-workers found that the introduction of  $\text{WO}_3$  into PTA/ $\text{TiO}_2$  films could further favor electron transfer by retarding recombination, leading to a higher photocurrent. The introduction of  $\text{WO}_3$ , together with the excellent electron mediator PTA into the  $\text{TiO}_2$  photoanode, provided a new route to boost the performance of DSSCs.<sup>[42]</sup>

Besides PTA, the introduction of some other Keggin-type POMs can also work similarly in photoanode. Xu and co-workers prepared a  $\text{H}_4\text{SiW}_{12}\text{O}_{40}/\text{ZnO}$  composite film by one-step electrodeposition method. Compared with the pristine  $\text{ZnO}$  film, the photo current and PCE of the DSSCs based on the composite film were significantly enhanced. The photoinduced electron transfer between POM and  $\text{ZnO}$  increased the efficient dissociation of excited electron-hole pairs.<sup>[43]</sup> In 2013, a series of POMs [ $\text{H}_x\text{MW}_{12}\text{O}_{40}$  ( $M=\text{P}$ ,  $x=3$ ;  $M=\text{Si, Ge}$ ,  $x=4$ )] were introduced into  $\text{ZnO}$  photoanodes by Li and co-workers. They investigated the effects of different Keggin-type  $\text{H}_x\text{MW}_{12}\text{O}_{40}$  on the performance of DSSCs. The results demonstrated that the presence of  $\text{H}_x\text{MW}_{12}\text{O}_{40}$  improved the performance of DSSCs efficiently by inhibiting the dark current, and the presence of  $\text{H}_3\text{PW}_{12}\text{O}_{40}$  gave the best PCE.<sup>[44]</sup>

As the development of POMs, it was found that the introduction of transition metal element of Co, Ni, Cu,

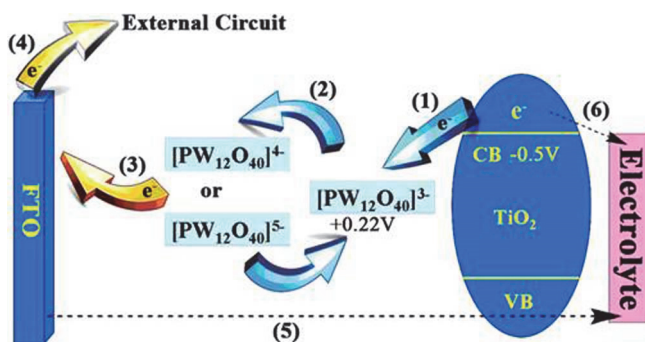


**Figure 3** Schematic diagram of electron transfer in the (PTA/TiO<sub>2</sub>)<sub>n</sub>-based DSSCs ( $n=1-5$ ) (From Ref. [41]).

Ru, etc. into the POMs could extend the light absorption to visible region, which was beneficial to the light harvest for solar cell. In 2014, Yang and co-workers prepared a novel SiW<sub>11</sub>Co/TiO<sub>2</sub> power by hydrothermal method. SiW<sub>11</sub>Co was also a kind of Keggin-type POMs and the absorption band and photoelectric response range was extended to the visible region compared with the commercial P25 powder, as shown in Figure 4. When SiW<sub>11</sub>Co/TiO<sub>2</sub> powder was mixed with the commercial P25 powder in a ratio of 1 : 1, the short circuit current increased by 63%.<sup>[45]</sup> Following this work, they further successfully prepared SiW<sub>11</sub>Cu/TiO<sub>2</sub> and SiW<sub>11</sub>Ni/TiO<sub>2</sub> powder by replacing the divalent metal Co with Cu or Ni. When SiW<sub>11</sub>Cu/TiO<sub>2</sub> or SiW<sub>11</sub>Ni/TiO<sub>2</sub> powder was mixed with P25 powder used as a photoanode, the PCE of 7.9% and 7.82% was obtained, which was much higher than that of pure P25-based photoanodes (~6%). The great enhancement of the device performance was attributed not only to the decrease of the charge carrier recombination but also the expanded absorption spectrum to the visible region.<sup>[19,46]</sup> Meanwhile, Wang and co-workers loaded TiO<sub>2</sub> on the surface of the tri-pyridine-ruthenium heteropolytungstate [Ru(bipy)<sub>3</sub>]<sub>2</sub>[SiW<sub>12</sub>O<sub>40</sub>]<sub>2</sub>•C<sub>2</sub>H<sub>5</sub>OH•8H<sub>2</sub>O (1@TiO<sub>2</sub>), which was mixed with P25 powder to serve as photoanode material in DSSCs. It was found that the transition metal ruthenium improved the performance of the cell and the short-circuit photocurrent density was 20.4% higher than that of the pure P25-based cells and 4.4% higher than that of the H<sub>4</sub>SiW<sub>12</sub>O<sub>40</sub>@TiO<sub>2</sub>-based cells.<sup>[47]</sup> In 2015, Wang and co-workers synthesized a di-vanadium-substituted Lindqvist-type POM [Cu(C<sub>12</sub>-H<sub>8</sub>N<sub>2</sub>)<sub>2</sub>]<sub>2</sub>[V<sub>2</sub>W<sub>4</sub>O<sub>19</sub>]<sub>2</sub>•4H<sub>2</sub>O (2). Ultraviolet photoelectron spectroscopy and density functional theoretical studies indicated that the energy level of **2** matched well with the conduction band of the TiO<sub>2</sub> and the absorption was extended to the visible region by Cu. When **2**-doped TiO<sub>2</sub> composites (2@TiO<sub>2</sub>) were mixed with P25 nanoparticles as photoanodes for DSSCs, the PCE of the DSSC assembled with **2**@TiO<sub>2</sub>/P25 photoanode was improved by 21.6% compared with that of the DSSC assembled with pure P25 photoanode. This enhancement of device performance was attributed to the smaller band gap of **2** than that of TiO<sub>2</sub> which accelerated electron transmission in the photoanode and better

UV/Visible absorption.<sup>[48]</sup> In 2016, a pure inorganic donor-acceptor (D-A) type polyoxometalate K<sub>6</sub>H<sub>4</sub>[ $\alpha$ -SiW<sub>9</sub>O<sub>37</sub>Co<sub>3</sub>(H<sub>2</sub>O)<sub>3</sub>]•17H<sub>2</sub>O (SiW<sub>9</sub>Co<sub>3</sub>)/reduced graphene oxide (RGO) nanocomposite was employed to DSSCs as a photoanode by Wang and co-workers. The SiW<sub>9</sub>Co<sub>3</sub>/RGO-3@P25 photoanode exhibited a wide spectrum (200–800 nm) and the performance of the cells was improved by 28.05% compared to the P25 photoanode. This increase in the photovoltaic performance was ascribed to the full spectrum properties of SiW<sub>9</sub>Co<sub>3</sub> and the quick and effective transformation of the photoinduced electrons of SiW<sub>9</sub>Co<sub>3</sub> on the graphene sheets.<sup>[49]</sup>

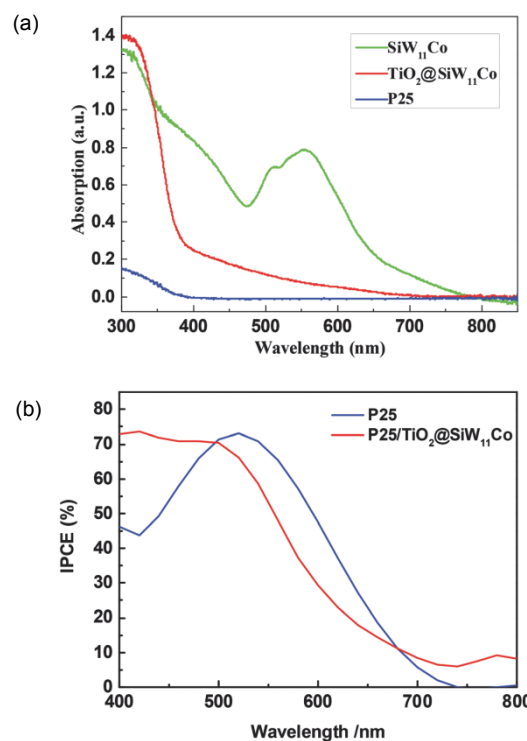


**Figure 4** (a) UV-vis spectra of SiW<sub>11</sub>Co, commercial P25 and TiO<sub>2</sub>/SiW<sub>11</sub>Co; (b) IPCE of dye-sensitized solar cells based on P25, TiO<sub>2</sub>/SiW<sub>11</sub>Co and P25-TiO<sub>2</sub>/SiW<sub>11</sub>Co. (From Ref. [45])

In addition, a Dawson-type heteropolyacid {P<sub>2</sub>Mo<sub>18</sub><sup>VI</sup>} and its two-electron heteropoly blue {P<sub>2</sub>Mo<sub>2</sub><sup>V</sup>Mo<sub>16</sub><sup>VI</sup>} were successfully doped into TiO<sub>2</sub> photoanode by a simple sol-gel method, the corresponding DSSCs achieved a significant enhanced performance due to the suppressed dark current and the increased electron lifetime. The working mechanism was very similar with that of Keggin-type POMs.<sup>[11]</sup>

POMs were usually used as photoanode together with TiO<sub>2</sub> or ZnO in DSSC. However, they can also be used as a photoanode alone by itself without TiO<sub>2</sub> or ZnO owing to their intrinsic semiconductor properties. In 2015, Yadollahi and co-workers synthesized a Keggin-type hybrid polyoxometalate [SiW<sub>11</sub>O<sub>39</sub>(Si(CH<sub>2</sub>)<sub>3</sub>-NH<sub>2</sub>)<sub>2</sub>O] (hybrid-POM) and the pristine hybrid-POM thin film was used as a photoanode in DSSC for the first time.<sup>[50]</sup> When fabricated with a D35 organic dye

as the sensitizer and an one-electron fast redox mediator cobalt complex, a promising improvement of photocurrent ( $J_{sc}$ ), IPCE values, and efficiency was achieved compared with that of the mesoporous titania structure. They attributed the improvement to that the crystalline structure of hybrid-POM led to an increase in the electron lifetime and a decrease in the recombination of the electrons with the redox mediator on the surface.<sup>[50]</sup> Pristine POMs could be used not only in DSSCs as photoanode materials, but also in the application of OPVs as an electron extraction layer. In 2013, Palilis and co-workers first extended the use of POMs (PTA) as an electron extraction layer in hybrid organic photovoltaic cells (HyOPVs) based on a bulk heterojunction P3HT:PCBM-61 active layer. As shown in Figure 5, PTA functioned as an efficient electron extraction/electron transport layer (EEL/ETL) due to its highly favorable optical properties and well energy level matching. Compared with the cells without electron extraction layer, an overall increase of ~40% in the short circuit photocurrent of the PW12 modified cell was achieved, while open circuit voltage increased from 0.61 up to 0.65 V and the fill factor raised from 0.36 to 0.41 resulting in a 70% improvement in the device PCE.<sup>[51]</sup> In 2015, Vasilopoulou and co-workers applied a series of POMs ( $H_4SiW_{12}O_{40}$ ,  $H_3PW_{12}O_{40}$ ,  $H_3PMo_{12}O_{40}$ ,  $H_5PV_2W_{10}O_{40}$ ,  $(NH_4)_6P_2W_{18}O_{62}$  and  $(NH_4)_6P_2Mo_{18}O_{62}$ ) with different low occupied molecular orbital (LUMO) in OPVs as electron extraction layers. They found that the POMs could be readily reduced at the interface with an Al electrode and that the degree of reduction was strongly affected by the position of their LUMO level which was related with the electronegative metal centers and the structure of POMs. The lower the LUMO level of POMs was, the better the device performance was. They attributed the enhancement to a large decrease of the electron injection/extraction barrier and improved electron transport.<sup>[52]</sup>

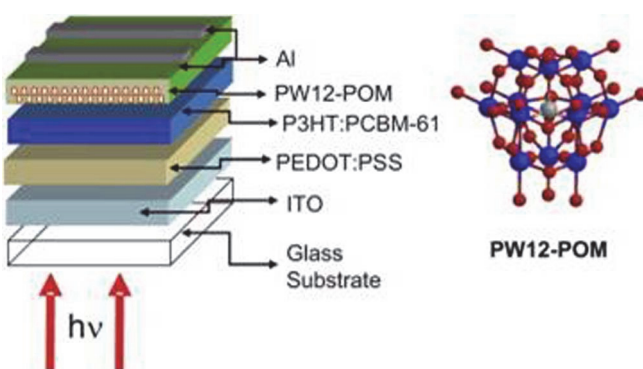


**Figure 5** Schematic architecture of the fabricated HyOPV and Keggin structure of the  $(PW_{12}O_{40})^{3-}$  anion of tungsten polyoxometalate. (From Ref. [51])

### POMs based light absorption materials

The high reactivity of POM molecule makes it possible to modify its structure at the molecular level. By

introducing organic chromophore or derivatives to the structure of POMs, the absorption of POMs can be expanded from the ultraviolet light to the visible/infrared light. These hybrid materials are a new kind of light absorption materials for solar cells. Indeed, great efforts have been devoted to developing organic/inorganic hybrid materials containing covalently linked POMs.

Peng and co-workers first applied POM-based materials in OPVs as light absorption materials in 2005. Hexamolybdate clusters were embedded through covalent bonds into the main chain of poly(phenylene acetylene)s. This hybrid polymer was soluble in organic solvents such as DMF and DMSO and showed intense absorption in the visible range. Simple single-layer photovoltaic cells with a device configuration of ITO/hybrid polymer/Ca was fabricated and a PCE of 0.15% has been obtained. The current density-voltage curve and the chemical structure of the hybrid polymer were shown in Figure 6.<sup>[53]</sup> In 2013, Ruhlmann and coworkers fabricated a 25-layer film containing  $\alpha_2\text{-Fe}^{III}P_2W_{17}O_{61}^{7-}$  polyanion and  $H_2TPhN(Me)_3P^4^+$  tetracationic porphyrin by a layer-by-layer self-assembly method, when it was assembled in photoelectrochemical cell which showed a 25 times higher photocurrent density than that for POM-free monolayer film. These results convincingly demonstrated the potential applications of POM-based organic/inorganic hybrids in molecular electronics and photonics.<sup>[54]</sup>

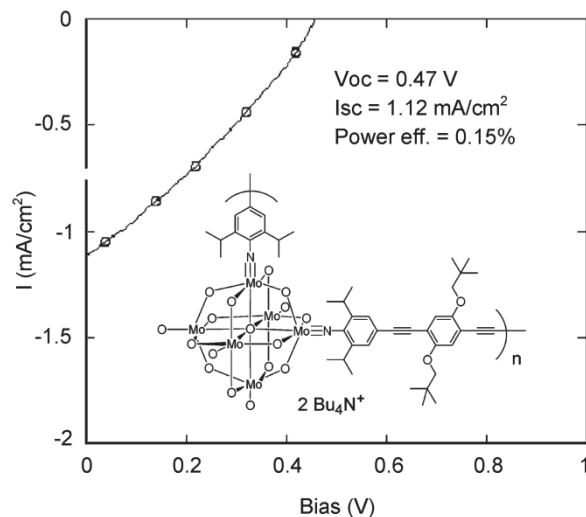


**Figure 6** Current density vs. voltage for an ITO/hybrid polymer/Ca device. (Reproduced from Ref. [53])

In 2013, Wang and co-workers synthesized a novel Keggin-type POMs  $[(CH_3)_4N]_5[PW_{11}O_{39}RhCH_2COOH] \cdot 6H_2O$  (PW<sub>11</sub>Rh-COOH, Figure 7) with the arm group ( $-COOH$ ) and it was the first POM-based photosensitizer explored in DSSCs. PW<sub>11</sub>Rh-COOH displayed a certain degree of photovoltaic response because of the good visible-light response and a PCE of 0.141% was obtained.<sup>[55]</sup> Following this work, they designed a sandwich-type germanotungstate  $[C(NH_2)_3]_{10-}$

[ $\text{Mn}_2\{\text{Sn}(\text{CH}_2)_2\text{COOH}\}_2(\text{B}-\alpha\text{-GeW}_9\text{O}_{34})_2\cdot 8\text{H}_2\text{O}$ ] [ $\text{Sn}(\text{CH}_2)_2\text{COOH}-\text{Mn}-\text{GeW}_9-\text{Mn}-\text{Sn}(\text{CH}_2)_2\text{COOH}$ ] functionalized by open chain carboxyethyltin, which was also used as a photosensitizer in DSSCs. The PCE of the solar cell was 0.22%, higher than that of  $\text{PW}_{11}\text{Rh-COOH}$ .<sup>[56]</sup> In 2016, Wang and co-workers synthesized three Keggin-type transition metal-substituted POMs,  $(n\text{C}_4\text{H}_9)_4\text{N}^+)_8\text{Na}_2[\text{SiW}_9\text{O}_{37}\{\text{Co}(\text{H}_2\text{O})_3\}] \cdot 11\text{H}_2\text{O}$  ( $\text{SiW}_9\text{Co}_3$ ),  $(n\text{C}_4\text{H}_9)_4\text{N}^+)_4[(\text{SiO}_4)\text{W}_{10}\text{Mn}^{\text{III}}_2\text{O}_{36}\text{H}_6] \cdot 1.5\text{CH}_3\text{CN} \cdot 2\text{H}_2\text{O}$  ( $\text{SiW}_{10}\text{Mn}^{\text{III}}_2$ ), and  $(n\text{C}_4\text{H}_9)_4\text{N}^+)_3.5\text{H}_5.5[(\text{SiO}_4)^-\text{W}_{10}\text{Mn}^{\text{III/IV}}_2\text{O}_{36}] \cdot 10\text{H}_2\text{O} \cdot 0.5\text{CH}_3\text{CN}$  ( $\text{SiW}_{10}\text{Mn}^{\text{III/IV}}_2$ ). They were used as photosensitizers for p-DSSCs utilizing  $\text{NiO}$  as a photoanode. These POMs were the first pure POM-based dyes used in p-DSSCs and all the three dyes showed good visible light absorption:  $\text{SiW}_9\text{Co}_3$  (350–663 nm),  $\text{SiW}_{10}\text{Mn}^{\text{III}}_2$  (350–800 nm) and  $\text{SiW}_{10}\text{Mn}^{\text{III/IV}}_2$  (350–800 nm), respectively. PCEs of 0.038%, 0.029%, and 0.027% were obtained, respectively, which were higher than that of coumarin 343 (0.017%).<sup>[57]</sup>

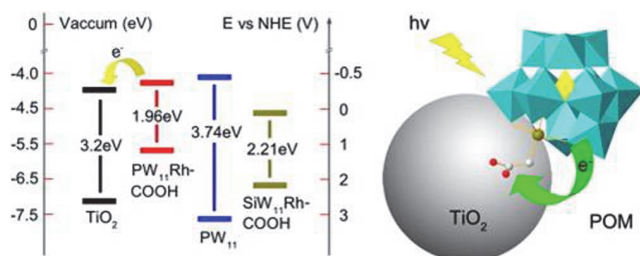


**Figure 7** Energy level diagram and scheme of POM sensitization mechanism. (From Ref. [54])

In 2013, Wang and co-workers first applied a spherical keplerate  $\{\text{W}_{72}\text{V}_{30}\}$  as the electron acceptor in a photovoltaic system and a water-soluble poly(*p*-phenylenevinylene) derivative was chosen as the electron donor. The composite film was fabricated by the LBL self-assembly method and showed significant photocurrent response. This work demonstrated that keplerate-type POMs ( $\{\text{W}_{72}\text{V}_{30}\}$ ) could be a promising electron-acceptor material and represented a promising strategy in designing polymer photovoltaic devices.<sup>[58]</sup> In 2015, Peng and co-workers synthesized two novel polythiophene-based hybrid conjugated polymers (**P2** and **P3**) containing different amounts of hexamolybdate clusters, which showed an absorption in the range of 400–700 nm. They fabricated OPVs with a device configuration of ITO/PEDOT:PSS/(**P2** or **P3**)/Ca/Al, and a PCE of 0.24% was obtained for **P2**, which was among the highest values reported for POM containing hybrid polymers.<sup>[59]</sup>

By combining of density functional theory (DFT) and time-dependent DFT (TDDFT) approaches, Su and co-workers investigated a series of POM-based organic-inorganic hybrids with different  $\pi$ -conjugated thiophene bridges as sensitizers for application in DSSCs (Figure 8). The results showed that the absorption spec-

tra were systematically broadened and red-shifted with increasing sizes of the  $\pi$ -conjugated spacer and the length of  $\pi$ -conjugation.<sup>[60]</sup> In 2016, they further investigated the UV-vis spectra and charge transfer (CT) characters of Zn-porphyrin-polyoxometalate hybrids with different  $\pi$ -conjugated bridges by DFT and TDDFT methods. They revealed a similar influence of  $\pi$ -conjugated bridges on sensitizers. The longer  $\pi$ -conjugated bridges and higher delocalization of systems would lead to the red shift and broadened absorption peak.<sup>[61]</sup> These theoretical studies provided valuable insight into the molecular design of novel POMs-based organic-inorganic hybrid for the further application in solar cells.

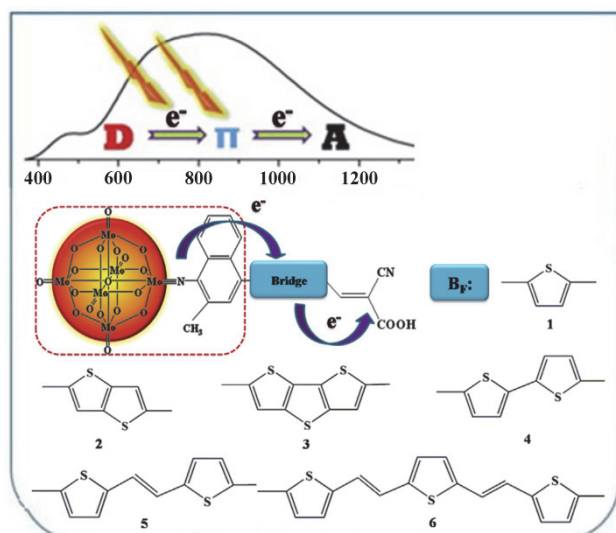


**Figure 8** Molecular structures of POM-based organic/inorganic hybrid materials **1**–**6**. (Reproduced from Ref. [60])

### POMs based electrolyte and hole extraction materials

The electron accepting ability makes POMs (especially for PTA) a good dopant to improve the ionic conductivity of solid electrolyte and retard the recombination of electron-hole pairs in DSSCs. What's more, some of the POMs have excellent redox properties, which can be oxidized and reduced at the same time, so they can form stable redox couple to replace  $\text{I}_3^-/\text{I}^-$  redox couple in DSSCs.

PTA was mixed with PVDF or PEO as a solid electrolyte in DSSCs to assist  $\text{I}_3^-/\text{I}^-$  redox couple. It was found that the PTA could inhibit the recombination of electron-hole pairs, greatly improve the efficiency and stability of the solar cells.<sup>[62–64]</sup> In 2007, Chen and co-workers successfully prepared a kind of novel composite polymeric gel comprising room-temperature ionic liquids (1-butyl-3-methyl-imidazolium-hexafluorophosphate,  $\text{BMImPF}_6^-$ ) and PTA in poly(2-hydroxyethyl methacrylate) matrix and employed it as a quasi-solid state electrolyte in DSSCs. Interestingly, they found that the ionic conductivity of the composite polymer electrolyte was effectively enhanced due to the addition of a

small amount of PTA. Unsealed devices employing the composite polymer electrolyte with a 3% content of PTA achieved a PCE of 1.68% under the irradiation of  $50 \text{ mW/cm}^2$  light intensity. After two months of work, the PCE of the device was maintained for 70%–75%.<sup>[65]</sup> In 2010, Sivakumar and co-workers prepared a new type of inorganic-organic hybrid solid state polymer electrolyte consisting of PTA impregnated poly-epichlorohydrin with iodine/iodide and  $\text{TiO}_2$  nanofiller for DSSCs. The PCE was found to be 5.48% and the stability of the fabricated dye sensitized solar cell was enhanced compared to the bare polymer electrolyte. It was attributed to the effect of PTA in impeding the back electron transfer, and increasing the ionic conductivity of the polymer electrolytes.<sup>[66]</sup>

In 2014, Wang and co-workers firstly employed two Keggin-type polyoxometalates ( $\text{K}_6\text{Co}^{\text{II}}\text{W}_{12}\text{O}_{40}$  and  $\text{K}_5\text{Co}^{\text{III}}\text{W}_{12}\text{O}_{40}$ ) as the redox couple in DSSCs. The redox potential value of the  $\text{Co}^{\text{III}}/\text{Co}^{\text{II}}$  couple matched with the potential of dye and the  $\text{TiO}_2$  conducting band. DSSCs with the POMs redox couple achieved relatively high  $V_{\text{oc}}$  (651 mV) and FF (0.549).<sup>[67]</sup> In addition, they firstly introduced two Anderson-type heteropolyanion-supported copper phenanthroline redox couples  $[\text{Al}(\text{OH})_6\text{Mo}_6\text{O}_{18}\{\text{Cu}(\text{phen})(\text{H}_2\text{O})_2\}_2][\text{Al}(\text{OH})_6\text{Mo}_6\text{O}_{18}\{\text{Cu}(\text{phen})(\text{H}_2\text{O})_2\}_2]$  (denoted as POM1-Cu-phen) and  $[\text{Cr}(\text{OH})_6\text{Mo}_6\text{O}_{18}\{\text{Cu}(\text{phen})(\text{H}_2\text{O})_2\}_2][\text{Cr}(\text{OH})_6\text{Mo}_6\text{O}_{18}\{\text{Cu}(\text{phen})(\text{H}_2\text{O})\text{Cl}\}_2]$  (denoted as POM2-Cu-phen) into DSSCs. The incorporation of Anderson-type heteropolyanions retarded the electron-hole recombination at the dyed  $\text{TiO}_2$  photoelectrode/electrolyte interface, facilitated the electron transfer from  $[\text{Cu}(\text{phen})_2]^+$  to dye cation, and tuned the redox potential of Cu(I/II) effectively. the short-circuit photocurrent, open-circuit voltage and the PCE were significantly increased by 2.2 times, 26.8% and 3.93 times, respectively, compared to the pristine copper phenanthroline redox couple. The working mechanism of DSSC with POM1/POM2-Cu-phen redox couple based electrolyte was shown in Figure 9.<sup>[68]</sup>

In the case of OPVs, similarly with the PTA which could be used as an electron extraction layer in OPVs owing to the energy level alignment at the cathode electrode, some POMs could be explored as hole extraction materials due to the energy level alignment at the anode electrode. Keggin phosphotungstic acid ( $\text{H}_3\text{PW}_{12}\text{O}_{40}$ , PMA) has been investigated as a hole extraction layer both in normal and inverted organic photovoltaic devices. The PMA layer could be fabricated by a spin coating process without any further treatment and the devices employing PMA as hole extraction layers exhibited better optical properties, less charge recombination and excellent long term stability compared with an evaporated  $\text{MoO}_3$  device.<sup>[69,70]</sup> Alaaeddine and co-workers introduced the use of the Dawson  $\text{K}_6[\text{P}_2\text{W}_{18}\text{O}_{62}]$  as an efficient hole extraction layer in conventional structured OPVs and the efficiency of the cell with  $\text{K}_6[\text{P}_2\text{W}_{18}\text{O}_{62}]$  was higher than that of the cell with PEDOT:PSS (2.6%

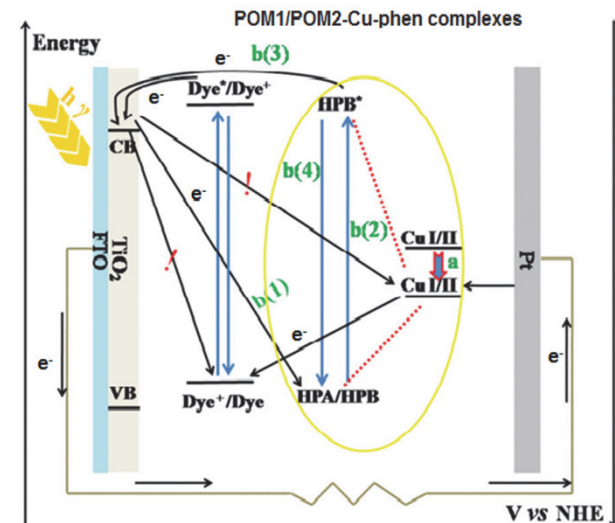


**Figure 9** A schematic working mechanism of DSSC with POM1/POM2-Cu-phen redox couples based electrolyte. ("...." represents covalent bond, "a" represents the positive shift of the redox potential of Cu(I/II).) (Reproduced from Ref. [68])

vs. 1.5%).<sup>[71]</sup> In 2015, Vasilopoulou and co-workers did some systematic research on the working mechanism of the POM-based hole extraction layer in OPVs. They selected two typical kinds of Keggin POMs (PTA and PMA) and their Dawson counterparts ( $\text{NH}_4)_6\text{P}_2\text{W}_{18}\text{O}_{62}$  and  $(\text{NH}_4)_6\text{P}_2\text{Mo}_{18}\text{O}_{62}$ , as the hole extraction materials in single junction and tandem OPVs. The schematic architecture of the OPV devices was shown in Figure 10. They found that all these materials exhibited a nearly similar extremely high work function (WF) of 6.0–6.2 eV, but differed on the position of their LUMO, which was heavily dependent on the type of the cluster (e.g., Keggin or Dawson) and the addenda atoms. It was observed that all POMs and especially those having a deep LUMO level lying below the highest occupied molecular orbital (HOMO) of the donor polymer were highly beneficial for device operation when used as hole extraction layers in OPVs. This was attributed to interfacial p-doping of the polymer donor which was caused by an electron transfer reaction between the polymer donor and the low LUMO POMs, resulting in negligible barrier hole extraction and enhanced hole transport rates.<sup>[72]</sup>

#### POMs based counter electrode (CE) materials

POMs have excellent electrocatalytic activity. In some electric catalytic processes, some POMs can carry out fast and reversible electron transfer process without degradation. This characteristic makes the POMs as a good supporting material for counter electrode in DSSCs and they are usually used together with conducting polymer, Pt or carbon materials.

In 2010, Almeida and co-workers synthesized two kinds of conducting polyanilines (PANI) doped with PTA and PMA (PANI-PTA and PANI-PMA), respectively and they utilized the PANI-POMs as new types of

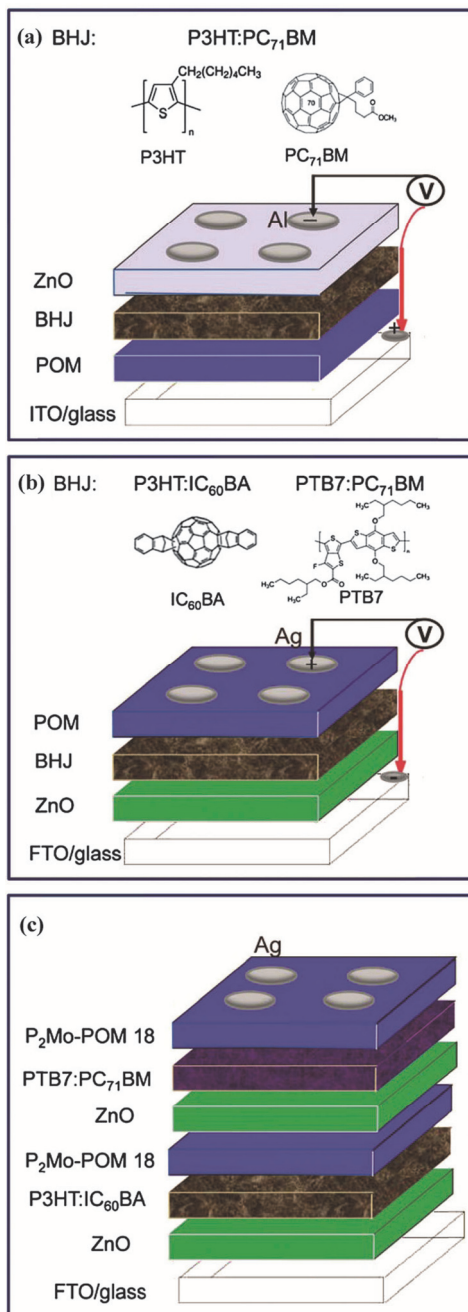


**Figure 10** Schematic architecture of the OPV devices with (a) the conventional structure ITO/POM/P3HT:PC71BM/ZnO/Al (OPV 1) and (b) the reverse structure FTO/ZnO/P3HT:IC60BA or PTB7:PC71BM/POM/Ag (OPV 2 and OPV 3). The chemical structures of the organic semiconductors used are also shown. (c) The structure of the tandem device. ( From Ref.[72])

counter electrodes in DSSCs. Due to the chemical oxidation of aniline by POMs, the conductivity values were improved from  $10^{-9}$  S•cm<sup>-1</sup> (for pristine PANI) to 0.1 S•cm<sup>-1</sup> (for PANI-PTA and PANI-PMA). When PANI-POMs were used as a counter electrode in DSSCs, the PCE of the devices were improved from 0.15% (for pristine PANI) to 0.21% (for PANI-PMA) and 0.29% (for PANI-PTA).<sup>[73]</sup> In 2012, Guo and co-workers fabricated a long-term stable Pt counter electrode modified by SiW<sub>9</sub>Al<sub>3</sub>/poly(diallyldimethylammonium chloride)-

based multilayer film by the electrochemical deposition method, which could markedly increase short-circuit photocurrent, open-circuit voltage and the PCE when used in DSSCs. The PCE increased from 5.62% to 6.76% and the architecture of the DSSC was shown in Figure 11.<sup>[74]</sup>

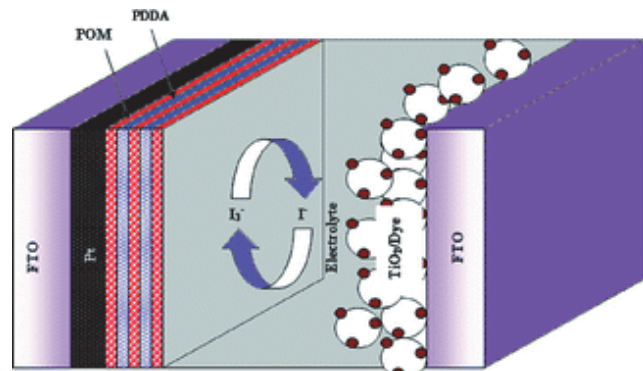


**Figure 11** Schematic architecture of the DSSC based on POM-modified counter electrode. ( From Ref. [74])

In 2013, Yuan and co-workers successfully prepared a POM-doped poly(3,4-ethylenedioxythiophene) (PEDOT) hybrid film counter electrode by electropolymerization in an environmentally friendly aqueous solution (Figure 12). The hybrid film presented a similar surface morphology to lotus leaf, the microstructure of which was a regular distribution of mastoid shapes. The dispersion of K<sub>8</sub>[SiW<sub>11</sub>O<sub>39</sub>]•13H<sub>2</sub>O (SiW<sub>11</sub>) improved the electrocatalytic activity and the efficiency of DSSCs based on hybrid film counter electrodes was almost as high as that of DSSCs with Pt counter electrodes.<sup>[75]</sup>

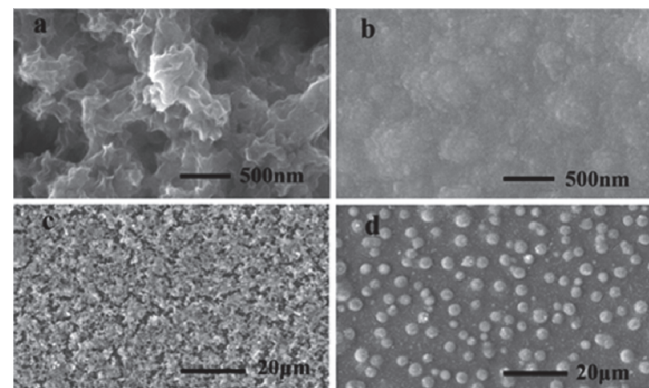


**Figure 12** FESEM images of (a, c) PEDOT-only film and (b, d) SiW<sub>11</sub>-PEDOT film. ( From Ref.[75])

In 2014, Sang and co-workers successfully synthesized two novel open-chain carboxyethyltin decorated sandwich-type germanotungstates (Sn(CH<sub>2</sub>)<sub>2</sub>COOH-Cu-GeW<sub>9</sub>-Cu-Sn(CH<sub>2</sub>)<sub>2</sub>COOH and Sn(CH<sub>2</sub>)<sub>2</sub>COOH-Co-GeW<sub>9</sub>-Co-Sn(CH<sub>2</sub>)<sub>2</sub>COOH). By Combining the high conductivity of single-walled carbon nanotubes and the catalytic activity of polyoxometallic derivatives, the electrocatalytic activity of single-walled carbon nano-

tubes toward triiodide reduction could be markedly increased. The photovoltaic performance was comparable to that of Pt electrodes. The architecture of DSSC based on POM-modified counter electrode and the current density-voltage curves were shown in Figure 13. This work provided a new strategy for the design of low cost and high efficiency of non-platinum counter electrode materials.<sup>[76]</sup>

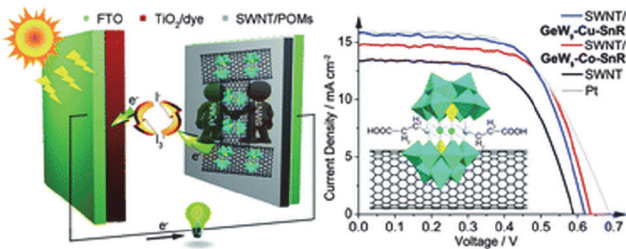


**Figure 13** Schematic architecture and the current density vs. voltage curves of the DSSCs based on POM-modified counter electrode. (From Ref. [76])

## Conclusions and Outlook

POMs are a versatile functional material and they can nearly act as all the roles in the architecture of DSSCs or OPVs. In this review, we have summarized the recent progress of POMs in DSSCs and OPVs classified by the building block in cells.

We first introduce the recent progress of POMs used as electronic interface materials. It reveals that POM-based electronic interface materials can act as a kind of electron shuttle and they have the ability to accept electron from the inorganic semiconductors and organic or metal complex sensitizers and then donate electron from reduced heteropoly blue to the external circuit. The working mechanism of POMs in DSSCs is shown in Figure 14. On one hand, the electron transfer process mediated by POMs efficiently improves the dissociation of excitons. On the other hand, the interfacial layers of POMs can reduce the backward electron transfer from  $\text{TiO}_2$  to electrolyte solution or sensitizers, which retards the electron recombination in DSSCs. Both roles that the POMs play are beneficial to enhancing the performance of DSSCs. For the working mechanism of the POMs in OPVs, the energy barrier between the active layer and the metal cathode can be reduced by POMs. The lower the LUMO level of POMs is, the smaller the energy barrier is and then the better the device performance is. In regard of the working mechanism and the development process of POM-based electronic interface materials, we can find the facts that the energy level of POMs could be adjusted by controlling their structures and the spectral absorption range of POMs can be tuned by varying transitional elements. Nevertheless, the molecular design rules of POM-based electronic interface materials are still not clear and systematic variations in the structures of POMs should be studied.

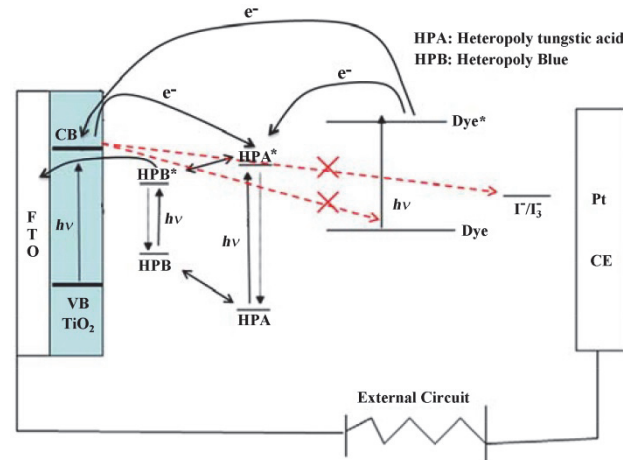


**Figure 14** Mechanism of electron flow through POM/ $\text{TiO}_2$  photoanode.

Secondly, in view of the POM-based light absorption materials, many novel light absorption materials have been synthesized based on POM-based inorganic-organic hybrid materials. They combine inorganic and organic features and may achieve synergistic effects. However, the explore of POM-based light absorption materials in optoelectronic field just starts, the photoelectric conversion efficiency of solar cells is very low and more researches are needed. Due to the abundant organic semiconductor molecules, there is a large space to develop the POMs hybrid materials as a kind of light absorption materials. Especially, much attention should be paid to the organic semiconductor with large  $\pi$ -conjugated structures according to Su and coworker's theoretical results.

Thirdly, owing to the excellent electron accepting ability, POMs can be good dopants to improve the ionic conductivity of solid electrolyte and adjust the hole collection energy barrier in OPVs. It is meaningful to explore the application of POMs into newly developing optoelectronic devices, such as tandem solar cell, perovskite solar cell, quantum dot solar cells, electroluminescent devices, etc.

Fourthly, the excellent electrocatalytic activity allows POMs to be used as a part of CE together with conducting polymer, Pt or carbon materials. POMs play the role of the improvement of the durability and electrocatalytic activity for CE. The types of POM-based CE are very few now and novel POMs with excellent electrocatalytic activity are desired.

What's more, in view of the fabrication of POM-based optoelectronic films, lots of easy and low-temperature processed methods are exploited, such as LBL Method, spin-coating technique, electrodeposition technique, etc. These easy and low-temperature processed methods are very suitable for practical applications in optoelectronic devices and flexible devices. While most of the common-used semiconductors need to be high-temperature processed during the device fab-

rification and POMs are usually used together with these semiconductors, such as TiO<sub>2</sub>, ZnO, Pt counter electrode, etc. Thus, the exploitation of pristine POMs with superior semiconductor properties is an interesting direction in future.

In brief, with the continuous development of new POMs derivatives and POM-based hybrid materials, the application of the POMs in solar energy conversion will become broader and more in-depth.

## Acknowledgement

This work was supported by the National Natural Science Foundation of China (Grant No. 51502058, 21571042), the China Postdoctoral Science Foundation (Grant No. 2015M570284), the Postdoctoral Foundation of Heilongjiang Province (LBH-TZ0604), and the Fundamental Research Funds for the Central Universities (Grant No. HIT AUGA5710055014).

## References

- [1] Long, D. L.; Burkholder, E.; Cronin, L. *Chem. Soc. Rev.* **2007**, *36*, 105.
- [2] Sadakane, M.; Moroi, S.; Iimuro, Y.; Izarova, N.; Kortz, U.; Hayakawa, S.; Kato, K.; Ogo, S.; Ide, Y.; Ueda, W.; Sano, T. *Chem.-Asian J.* **2012**, *7*, 1331.
- [3] Choi, J. H.; Kang, T. H.; Song, J. H.; Bang, Y.; Song, I. K. *Catal. Commun.* **2014**, *43*, 155.
- [4] Putaj, P.; Lefebvre, F. *Coord. Chem. Rev.* **2011**, *255*, 1642.
- [5] Izarova, N. V.; Pope, M. T.; Kortz, U. *Angew. Chem., Int. Ed.* **2012**, *51*, 9492.
- [6] Nyman, M.; Burns, P. C. *Chem. Soc. Rev.* **2012**, *41*, 7354.
- [7] Pope, M. T.; Müller, A. *Angew. Chem., Int. Ed. Engl.* **1991**, *30*, 34.
- [8] Marci, G.; Garcia-López, E. I.; Palmisano, L. *Eur. J. Inorg. Chem.* **2014**, *21*.
- [9] Yoon, Y. *M.S. Dissertation*, Emporia State University, Emporia, **1994**.
- [10] Sivakumar, R.; Thomas, J.; Yoon, M. *J. Photochem. Photobiol., C* **2012**, *13*, 277.
- [11] Chen, L.; Sang, X.-J.; Li, J.-S.; Shan, C.-H.; Chen, W.-L.; Su, Z.-M.; Wang, E.-B. *Inorg. Chem. Commun.* **2014**, *47*, 138.
- [12] Himeno, S.; Takamoto, M.; Ueda, T. *J. Electroanal. Chem.* **2000**, *485*, 49.
- [13] Himeno, S.; Takamoto, M.; Ueda, T.; Santo, R.; Ichimura, A. *Electroanalysis* **2004**, *16*, 656.
- [14] Takamoto, M.; Ueda, T.; Himeno, S. *J. Electroanal. Chem.* **2002**, *521*, 132.
- [15] Tan, C.; Liu, N.; Yu, B.; Zhang, C.; Bu, W.; Liu, X.; Song, Y.-F. *J. Mater. Chem. C* **2015**, *3*, 2450.
- [16] He, P.; Xu, B.; Xu, X.; Song, L.; Wang, X. *Chem. Sci.* **2016**, *7*, 1011.
- [17] Yang, H.; Li, J.; Zhang, H.; Lv, Y.; Gao, S. *Microporous Mesoporous Mater.* **2014**, *195*, 87.
- [18] Xuan, W. J.; Botuha, C.; Hasenkopf, B.; Thorimbert, S. *Chem. - Eur. J.* **2015**, *21*, 16512.
- [19] Jiang, Y.; Yang, Y.; Qiang, L.; Fan, R.; Li, L.; Ye, T.; Na, Y.; Shi, Y.; Luan, T. *Phys. Chem. Chem. Phys.* **2015**, *17*, 6778.
- [20] Xu, S. S.; Chen, W. L.; Wang, Y. H.; Li, Y. G.; Liu, Z. J.; Shan, C. H.; Su, Z. M.; Wang, E. B. *Dalton Trans.* **2015**, *44*, 18553.
- [21] Wang, L.; Yu, K.; Zhou, B. B.; Su, Z. H.; Gao, S.; Chu, L. L.; Liu, J. R. *Dalton Trans.* **2014**, *43*, 6070.
- [22] Tong, X.; Thangadurai, V. *J. Phys. Chem. C* **2015**, *119*, 7621.
- [23] Zhang, Y.; Bo, X.; Nsabimana, A.; Munyentwali, A.; Han, C.; Li, M.; Guo, L. *J. Biosens. Bioelectron.* **2015**, *66*, 191.
- [24] Graham, K.; Douglas, F. J.; Mathieson, J. S.; Moggach, S. A.; Schnack, J.; Murrie, M. *Dalton Trans.* **2011**, *40*, 12271.
- [25] Yu, K.; Zhou, B.; Yu, Y.; Su, Z.; Wang, C.; Wang, C.; Gao, S.; Chen, Y. *Inorg. Chim. Acta* **2012**, *384*, 8.
- [26] Liu, L.-Q.; Zhang, G.-C.; He, B.-T.; Huang, F. *Chin. J. Chem.* **2015**, *33*, 902.
- [27] Wu, F.; Liu, H.-T.; Lee, L.; Chen, T.; Wang, M.; Zhu, L. *Chin. J. Chem.* **2015**, *33*, 925.
- [28] Dolbecq, A.; Dumas, E.; Mayer, C. D. R.; Mialane, P. *Chem. Rev.* **2010**, *110*, 6009.
- [29] Douvas, A. M.; Makarona, E.; Glezos, N.; Argitis, P.; Mielczarski, J. A.; Mielczarski, E. *ACS Nano* **2008**, *2*, 733.
- [30] Hiskia, A.; Mylonas, A.; Papaconstantinou, E. *Chem. Soc. Rev.* **2001**, *30*, 62.
- [31] Radhakrishnan, R.; Thomas, J.; Yoon, M. *J. Photochem. Photobiol., C* **2012**, *4*, 277.
- [32] Song, F.Y.; Ding, Y.; Zhao, C. C. *Acta Chim. Sinica* **2014**, *72*, 133.
- [33] Walsh, J. J.; Bond, A. M.; Forster, R. J.; Keyes, T. E. *Coord. Chem. Rev.* **2016**, *306*, 217.
- [34] Ji, Y. C.; Huang, L. J.; Hu, J.; Streb, C.; Song, Y. F. *Energy Environ. Sci.* **2015**, *8*, 776.
- [35] Genovese, M.; Lian, K. *Curr. Opin. Solid State Mater. Sci.* **2015**, *19*, 126.
- [36] Kourasi, M.; Wills, R. G. A.; Shah, A. A.; Walsh, F. C. *Electrochim. Acta* **2014**, *127*, 454.
- [37] Yang, W.; Gao, L. H.; Wang, K. Z. *Polyhedron* **2014**, *82*, 80.
- [38] Herrmann, S.; Ritchie, C.; Streb, C. *Dalton Trans.* **2015**, *44*, 7092.
- [39] Parayil, S. K.; Lee, Y. M.; Yoon, M. *Electrochim. Commun.* **2009**, *11*, 1211.
- [40] Wang, S. M.; Liu, L.; Chen, W. L.; Wang, E. B.; Su, Z. M. *Dalton Trans.* **2013**, *42*, 2691.
- [41] Wang, S. M.; Liu, L.; Chen, W. L.; Su, Z. M.; Wang, E. B.; Li, C. *Ind. Eng. Chem. Res.* **2014**, *53*, 150.
- [42] Li, W. Z.; Jin, H. S.; Hu, H. S.; Li, J.; Yang, Y. H. *Electrochim. Acta* **2015**, *153*, 499.
- [43] Luo, X.; Li, F.; Xu, B.; Sun, Z.; Xu, L. *J. Mater. Chem.* **2012**, *22*, 15050.
- [44] Li, J.; Sang, X.; Chen, W.; Qin, C.; Wang, S.; Su, Z.; Wang, E. *Eur. J. Inorg. Chem.* **2013**, 1951.
- [45] Li, L.; Yang, Y.; Fan, R.; Wang, X.; Zhang, Q.; Zhang, L.; Yang, B.; Cao, W.; Zhang, W.; Wang, Y.; Ma, L. *Dalton Trans.* **2014**, *43*, 1577.
- [46] Jiang, Y.; Yang, Y.; Qiang, L.; Fan, R.; Ning, H.; Li, L.; Ye, T.; Yang, B.; Cao, W. *J. Power Sources* **2015**, *278*, 527.
- [47] Shan, C. H.; Sang, X. J.; Zhang, H.; Li, J. S.; Chen, W. L.; Su, Z. M.; Wang, E. B. *Inorg. Chem. Commun.* **2014**, *50*, 13.
- [48] Xu, S. S.; Chen, W. L.; Wang, Y. H.; Li, Y. G.; Liu, Z. J.; Shan, C. H.; Su, Z. M.; Wang, E. B. *Dalton Trans.* **2015**, *44*, 18553.
- [49] Shan, C. H.; Zhang, H.; Chen, W. L.; Su, Z. M.; Wang, E. B. *J. Mater. Chem. A* **2016**, *4*, 3297.
- [50] Karimian, D.; Yadollahi, B.; Zendehdel, M.; Mirkhani, V. *RSC Adv.* **2015**, *5*, 76875.
- [51] Palilis, L. C.; Vasilopoulou, M.; Douvas, A. M.; Georgiadou, D. G.; Kennou, S.; Stathopoulos, N. A.; Constantoudis, V.; Argitis, P. *Sol. Energy Mater. Sol. Cells* **2013**, *114*, 205.
- [52] Vasilopoulou, M.; Douvas, A. M.; Palilis, L. C.; Kennou, S.; Argitis, P. *J. Am. Chem. Soc.* **2015**, *137*, 6844.
- [53] Lu, M.; Xie, B.; Kang, J.; Chen, F.-C.; Yang, Y.; Peng, Z. *Chem. Mater.* **2005**, *17*, 402.
- [54] Ahmed, I.; Farha, R.; Goldmann, M.; Ruhmann, L. *Chem. Commun.* **2013**, *49*, 496.
- [55] Li, J.-S.; Sang, X.-J.; Chen, W.-L.; Zhang, L.-C.; Su, Z.-M.; Qin, C.; Wang, E.-B. *Inorg. Chem. Commun.* **2013**, *38*, 78.
- [56] Sang, X. J.; Li, J. S.; Zhang, L. C.; Wang, Z. J.; Chen, W. L.; Zhu, Z. M.; Su, Z. M.; Wang, E. B. *ACS Appl. Mater. Interfaces* **2014**, *6*, 7876.
- [57] Guo, X. W.; Li, J. S.; Sang, X. J.; Chen, W. L.; Su, Z. M.; Wang, E. B. *Chem. Eur. J.* **2016**, *22*, 3234.

- [58] Jin, G.; Wang, S.-M.; Chen, W.-L.; Qin, C.; Su, Z.-M.; Wang, E.-B. *J. Mater. Chem. A* **2013**, *1*, 6727.
- [59] Wang, R. X.; Li, Y.; Shetye, K.; Dutta, T.; Jin, L.; Li, S. H.; Peng, Z. H. *Eur. J. Inorg. Chem.* **2015**, 656.
- [60] Wang, J.; Li, H.; Ma, N.-N.; Yan, L.-K.; Su, Z.-M. *Dyes Pigm.* **2013**, *99*, 440.
- [61] Wu, H. N.; Zhang, T.; Wu, C. X.; Guan, W.; Yan, L. K.; Su, Z. M. *Dyes Pigm.* **2016**, *130*, 168.
- [62] Anandan, S.; Pitchumani, S.; Muthuraaman, B.; Maruthamuthu, P. *Sol. Energy Mater. Sol. Cells* **2006**, *90*, 1715.
- [63] Anandan, S.; Sivakumar, R. *Phys. Status Solidi A* **2009**, *206*, 343.
- [64] Akhtar, M. S.; Cheralathan, K. K.; Chun, J.-M.; Yang, O. B. *Electrochim. Acta* **2008**, *53*, 6623.
- [65] Chen, D.; Zhang, Q.; Wang, G.; Zhang, H.; Li, J. *Electrochem. Commun.* **2007**, *9*, 2755.
- [66] Sivakumar, R.; Akila, K.; Anandan, S. *Curr. Appl. Phys.* **2010**, *10*, 1255.
- [67] Yuan, C.-C.; Wang, S. M.; Chen, W. L.; Liu, L.; Zhang, Z. M.; Lu, Y.; Su, Z. M.; Zhang, S. W.; Wang, E. B. *Inorg. Chem. Commun.* **2014**, *46*, 89.
- [68] Yuan, C. C.; Wang, S. M.; Chen, W. L.; Liu, L.; Qin, C.; Su, Z. M.; Wang, E. B. *Dalton Trans.* **2014**, *43*, 1493.
- [69] Jia, X.; Shen, L.; Yao, M.; Liu, Y.; Yu, W.; Guo, W.; Ruan, S. *ACS Appl. Mater. Interfaces* **2015**, *7*, 5367.
- [70] Zhu, Y.; Yuan, Z.; Cui, W.; Wu, Z.; Sun, Q.; Wang, S.; Kang, Z.; Sun, B. *J. Mater. Chem. A* **2014**, *2*, 1436.
- [71] Alaaeddine, M.; Zhu, M.; Fichou, D.; Izzet, G.; Rault, J. E.; Barrett, N.; Proust, A.; Tortech, L. *Inorg. Chem. Front.* **2014**, *1*, 682.
- [72] Vasilopoulou, M.; Polydorou, E.; Douvas, A. M.; Palilis, L. C.; Kennou, S.; Argitis, P. *Energy Environ. Sci.* **2015**, *8*, 2448.
- [73] Almeida, L. C. P.; Gonçalves, A. D.; Benedetti, J. E.; Miranda, P. C. M. L.; Passoni, L. C.; Nogueira, A. F. *J. Mater. Sci.* **2010**, *45*, 5054.
- [74] Guo, S. S.; Qin, C.; Li, Y. G.; Lu, Y.; Su, Z. M.; Chen, W. L.; Wang, E. B. *Dalton Trans.* **2012**, *41*, 2227.
- [75] Yuan, C.; Guo, S.; Wang, S.; Liu, L.; Chen, W.; Wang, E. *Ind. Eng. Chem. Res.* **2013**, *52*, 6694.
- [76] Sang, X.-J.; Li, J.-S.; Zhang, L.-C.; Zhu, Z.-M.; Chen, W.-L.; Li, Y.-G.; Su, Z.-M.; Wang, E.-B. *Chem. Commun.* **2014**, *50*, 14678.

(Pan, B.; Fan, Y.)